# Supplementary Information

# Remodeling of Conformational Dynamics Enhances Catalytic Activities of M1 Zinc-metallopeptidases from Lanthipeptide Biosynthesis

Chang Zhao,[1,3] Wangjian Sheng,[2,3] Ying Wang,[2] Jie Zheng,[2] Xiangqian Xie,[2] Yong Liang,[2] Wanqing Wei,[2*] Rui Bao[1*] and Huan Wang [2*]

[1]Center of Infectious Diseases, State Key Laboratory of Biotherapy, West China Hospital, Sichuan University and Collaborative Innovation Center, Chengdu, China

[2]State Key Laboratory of Coordination Chemistry, Chemistry and Biomedicine Innovation Center of Nanjing University, Jiangsu Key Laboratory of Advanced Organic Materials, School of Chemistry and Chemical Engineering, Nanjing University, Nanjing 210093, China

[3]These authors contributed equally: Chang Zhao, Wangjian Sheng

*e-mail: wanghuan@nju.edu.cn; baorui@scu.edu.cn; wanqwei@163.com

**List of supplementary figures and tables:**

**Supplementary Table 1.** Primers used in this study

| Primer | Sequence (5'-3') |
|---|---|
| AplA BamHI F | TGCTGGATCCAGTCCAGGAAATTCTGGAACTGCAAGAACTGCC |
| AplA HindIII R | TGCTAAGCTTTTAACAGTTGGACCAGGTAAAGGAACTCGGCCAAC |
| AplKC NdeI F | AGCTCATATGGTTCTGGATACCCGTTATATTCGCTTTTGCCGTC |
| AplKC XhoI R | AGCTCTCGAGTTATTCTTCAGAATCGGCACCCGCGGAG |
| AplP NdeI F | GATTCATATGGTGACCCGTCCGGAGGC |
| AplP XhoI R | GTATCTCGAGTTAACGACCCGGCGCCACC |
| $AplP_{R98E}$ F | AGCCGTAGCGGTGAAGGCCTGAGCCGT |
| $AplP_{R98E}$ R | ACGGCTCAGGCCTTCACCGCTACGGCT |
| $AplP_{A368E}$ F | GATACCGATGCGGAGCTGCGTTTCGAC |
| $AplP_{A368E}$ R | GTCGAAACGCAGCTCCGCATCGGTATC |
| $AplP_{A779R}$ F | CGTTGGCCGGCGCGCCAGGCGCACCAC |
| $AplP_{A779R}$ R | GTGGTGCGCCTGGCGCGCCGGCCAACG |
| EryP NdeI F | AGCTCATATGGCTCCGCCGAACCTGACCCG |
| EryP XhoI R | AGCTGCTCTCGAGTCAGCTACGGTCAAACTCACGCGC |
| $EryP_{E307Q}$ F | ACCGTGCTGCACCAGATGGCGCACATG |
| $EryP_{E307Q}$ R | CATGTGCGCCATCTGGTGCAGCACGGT |
| $EryP_{E384A}$ F | CTGCAGGCGGTGGCAGTTAACTTTGAT |
| $EryP_{E384A}$ R | ATCAAAGTTAACTGCCACCGCCTGCAG |
| $EryP_{Y392F}$ F | GATGGTATCACCTTTGCGAAGGGCGCG |
| $EryP_{Y392F}$ R | CGCGCCCTTCGCAAAGGTGATACCATC |
| $EryP_{E802A}$ F | CGTCGTAGCAGCGCACGTGCGCAGCCG |
| $EryP_{E802A}$ R | CGGCTGCGCACGTGCGCTGCTACGACG |
| $EryP_{E802R}$ F | CGTCGTAGCAGCCGTCGTGCGCAGCCG |
| $EryP_{E802R}$ R | CGGCTGCGCACGACGGCTGCTACGACG |

**Supplementary Table 2.** Data collection and refinement statistics of EryP and $EryP_{E802R}$

| Parameters | SeMet | *closed* | *intermediate* | *open* | $EryP_{E802R}$ |
|---|---|---|---|---|---|
| **Data collection** | | | | | |
| Wavelength (Å) | 0.97918 | 0.97918 | 0.97918 | 0.97930 | 0.9785 |
| Space group | $P4_12_1$ 2 | $P4_32_12$ | $P12_11$ | $P2_12_12_1$ | $P12_11$ |
| Cell dimensions | | | | | |
| a, b, c (Å) | 153.75<br>153.75<br>97.64 | 153.58<br>153.58<br>98.42 | 91.42<br>66.63<br>153.74 | 58.818<br>111.577<br>156.089 | 58.909<br>143.583<br>60.58 |
| α, β, γ (°) | 90 90 90 | 90 90 90 | 90 93.41 90 | 90 90 90 | 90 114.76 90 |
| Resolution (Å) | 82.42 - 2.56<br>(2.63 - 2.56) * | 39.09 - 1.90<br>(1.93 - 1.90) * | 37.74 - 1.80<br>(1.85 - 1.80) * | 36.18 -2.66<br>(2.76- 2.66) * | 19.57 - 1.77<br>(1.83- 1.77) * |
| Rmerge | 0.384(3.052) | 0.124(0.750) | 0.048(0.443) | 0.205(0.775) | 0.073(0.293) |
| Completeness (%) | 100.0 (100.0) | 100.0 (99.8) | 98.9(91.6) | 99.37 (97.44) | 99.7(99.8) |
| Mean I/σ (I) | 12.8(1.8) | 25.2(6.1) | 16.4(2.1) | 8.74(1.68) | 16.1(5.0) |
| **Refinement** | | | | | |
| Resolution (Å) | | 1.90 | 1.80 | 2.66 | 1.77 |
| Rwork/Rfree | | 15.38/18.14 | 19.00/21.02 | 20.18/21.58 | 13.61/17.19 |
| No. reflections | | 92586<br>(9138) | 169146<br>(15534) | 29991<br>(2859) | 88415<br>(8837) |
| RMSD | | | | | |
| bond lengths (Å) | | 0.022 | 0.014 | 0.020 | 0.021 |
| bond angles (°) | | 1.79 | 1.20 | 1.68 | 1.78 |
| No. atoms | | | | | |
| Protein | | 6808 | 13318 | 6720 | 6806 |
| Ligand/ion | | 24 | 2 | 1 | 13 |
| water | | 796 | 1058 | 131 | 1367 |
| B-factors | | | | | |
| Protein | | 27.23 | 42.36 | 52.81 | 14.88 |
| Ligand/ion | | 36.56 | 37.44 | 32.11 | 23.14 |
| water | | 36.70 | 45.67 | 45.08 | 26.28 |
| Ramachandran plot | | | | | |
| Favored | | 97.67 | 98.28 | 98.02 | 97.90 |
| Allowed | | 2.33 | 1.72 | 1.98 | 2.10 |
| Dis-allowed | | 0 | 0 | 0 | 0 |

Data were collected from a single crystal. *Values in parentheses are for highest-resolution shell.

**Supplementary Table 3.** Detailed MS data of Figure 6a.

| Species | Sequence | Predicted Mass/Da | Observed Mass/Da |
|---|---|---|---|
| **$AplA_{LP}$(-19)** | $His_6$-VQE | 1855.86 | 1855.57 |
| **$AplA_{LP}$(-17)** | $His_6$-VQEIL | 2082.18 | 2082.8 |
| **$AplA_{LP}$(-16)** | $His_6$-VQEILE | 2211.3 | 2211.74 |
| **$AplA_{LP}$(-14)** | $His_6$-VQEILELQ | 2452.59 | 2452.97 |
| **$AplA_{LP}$(-13)** | $His_6$-VQEILELQE | 2581.7 | 2581.81 |
| **$AplA_{LP}$(-11)** | $His_6$-VQEILELQELP | 2791.98 | 2791.96 |
| **$AplA_{LP}$(-5)** | $His_6$-VQEILELQELPSASATE | 3338.51 | 3338.46 |
| **$AplA_{cyc}$** | $His_6$-VQEILELQELPSASATEDMPL-$AplA_{cyc}$-cp | 5998.58 | 5998.02 |

**Supplementary Table 4.** Detailed MS data of Figure 6b.

| Species | Sequence | Predicted $[M+Na]^+$ Mass/Da | Observed$[M+Na]^+$ Mass/Da |
|---|---|---|---|
| **$AplA_{CP}$(-1)** | L-$AplA_{cyc-CP}$ | 2356.03 | 2355.53 |
| **$AplA_{CP}$(-2)** | PL-$AplA_{cyc-CP}$ | 2453.08 | 2452.59 |
| **$AplA_{CP}$(-3)** | MPL-$AplA_{cyc-CP}$ | 2584.12 | 2583.57 |
| **$AplA_{CP}$(-4)** | DMPL-$AplA_{cyc-CP}$ | 2699.15 | 2698.72 |
| **$AplA_{CP}$(-5)** | EDMPL-$AplA_{cyc-CP}$ | 2828.19 | 2828.49 |
| **$AplA_{CP}$(-6)** | TEDMPL-$AplA_{cyc-CP}$ | 2929.24 | 2928.57 |
| **$AplA_{LP}$(-13)** | $His_6$-VQEILELQE | 2603.18 | 2602.57 |
| **$AplA_{LP}$(-11)** | $His_6$-VQEILELQELP | 2813.31 | 2813.63 |
| **$AplA_{LP}$(-10)** | $His_6$-VQEILELQELPS | $[M+H]^+$= 2877.3543 | $[M+H]^+$= 2877.562 |

A)

| Lanthipeptide | Strain | Gene | Accession number | Genome coordinates |
|---|---|---|---|---|
| Erythreapeptin | *Saccharopolyspora erythraea* NRRL 2338 | *eryP* | WP_009950696.1 | NC_009142.1 1484009-1486591 (-) |
| | | *eryKC* | WP_009949110.1 | NC_009142.1 4798016-4800550 (+) |
| | | *eryA* | WP_009949109.1 | NC_009142.1 4800618-4800758 (+) |
| | | *ramA* | WP_009949108.1 | NC_009142.1 4800854-4802512 (+) |
| | | *ramB* | WP_009949106.1 | NC_009142.1 4802509-4804218 (+) |

B)

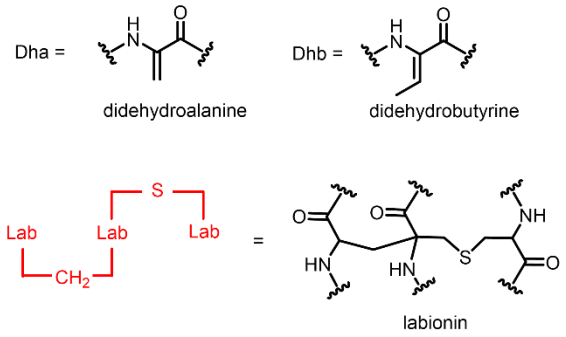


**Supplementary Figure 1.** (A) Genetic information of the *ery* BGC and the *eryP* gene in the genome of *Saccharopolyspora erythraea* NRRL 2338. (B) Chemical structures of Dha, Dhb and labionin motifs in erythreapeptin.

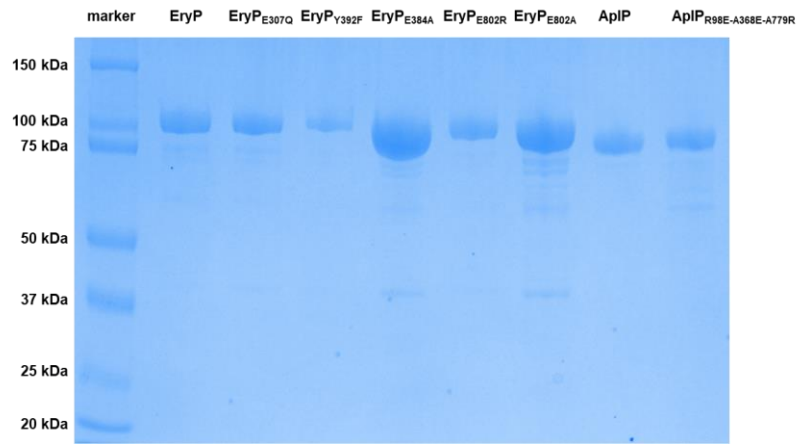


**Supplementary Figure 2.** SDS-PAGE analysis of enzymes investigated in this study. M.W. of EryP is 96.2 kDa, and M.W. of AplP is 90.7 kDa.

| Substrate | [$CaCl_2$] (mM) | $K_m$ (mM) | $V_{max}$ (μM·min$^{-1}$) | $k_{cat}$(min$^{-1}$) | $k_{cat}/K_m$ (min$^{-1}$mM$^{-1}$) |
|---|---|---|---|---|---|
| **Ala-*p*NA** | none | 36 ± 5 | 81 ± 9 | 81 | 2.2 |
| | 1.0 | 5.2 ± 0.1 | 57 ± 1 | 57 | 11 |
| **Leu-*p*NA** | none | 1.6 ± 0.1 | 18 ± 1 | 18 | 11 |
| | 1.0 | 2.6 ± 0.1 | 89 ± 4 | 89 | 35 |
| **Pro-*p*NA** | none | 11 ± 1 | 9.5 ± 0.6 | 9.6 | 0.87 |
| | 1.0 | 5.4 ± 0.4 | 16 ± 1 | 16 | 3.0 |

**Supplementary Figure 3.** Catalytic efficiency of EryP toward Ala-*p*NA, Pro-*p*NA and Leu-*p*NA. Assay conditions: 1.0 μM EryP was incubated with Ala-*p*NA (100 μM to 10 mM) or Pro-*p*NA (100 μM to 10 mM) or Leu-*p*NA (10 μM to 1.0 mM) in 20 mM Tris buffer, *p*H 8.0, at 37 °C. Error values indicate standard deviation of three independent replicates.

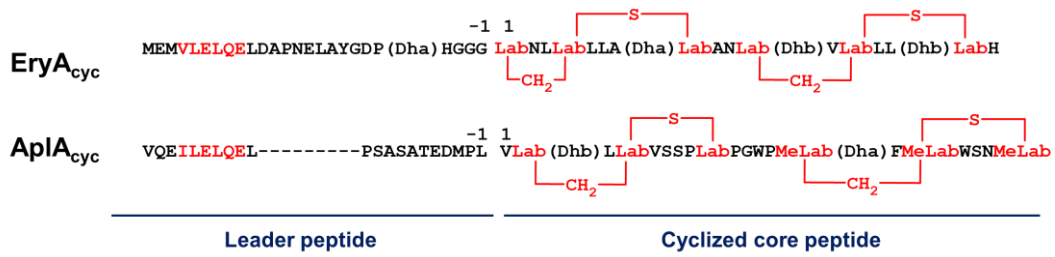


**Supplementary Figure 4.** Structural comparison between $EryA_{cyc}$ and $AplA_{cyc}$.

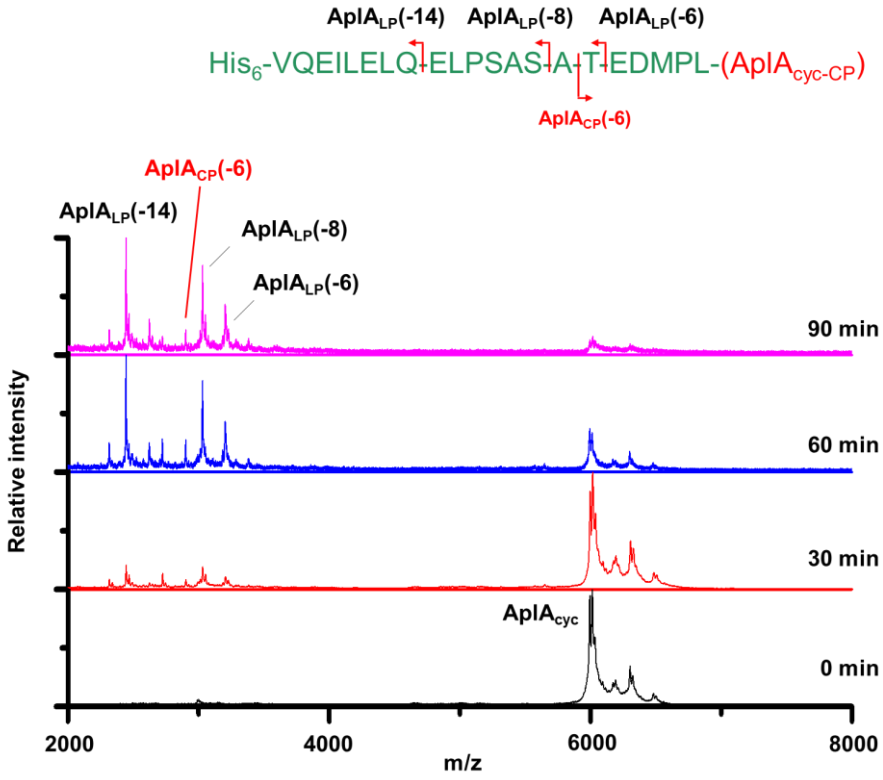


| Species | Sequence | Predicted Mass/Da | Observed Mass/Da |
|---|---|---|---|
| AplA$_{LP}$(-14) | His$_6$-VQEILELQ | 2452.59 | 2452.89 |
| AplA$_{LP}$(-8) | His$_6$-VQEILELQELPSAS | 3036.43 | 3036.31 |
| AplA$_{LP}$(-6) | His$_6$-VQEILELQELPSASAT | 3208.52 | 3208.46 |
| AplA$_{CP}$(-6) | TEDMPL-AplA$_{cyc-CP}$ | 2889.19 | 2889.88 |

**Supplementary Figure 5.** EryP cleaves AplA$_{cyc}$ peptide as an endopeptidase at multiple sites, as determined by MALDI-TOF analysis. Assay conditions: 100 μM AplA$_{cyc}$ peptide and 1.0 μM EryP were incubated in 20 mM Tris buffer, *p*H 8.0, at 37 °C for indicated time.

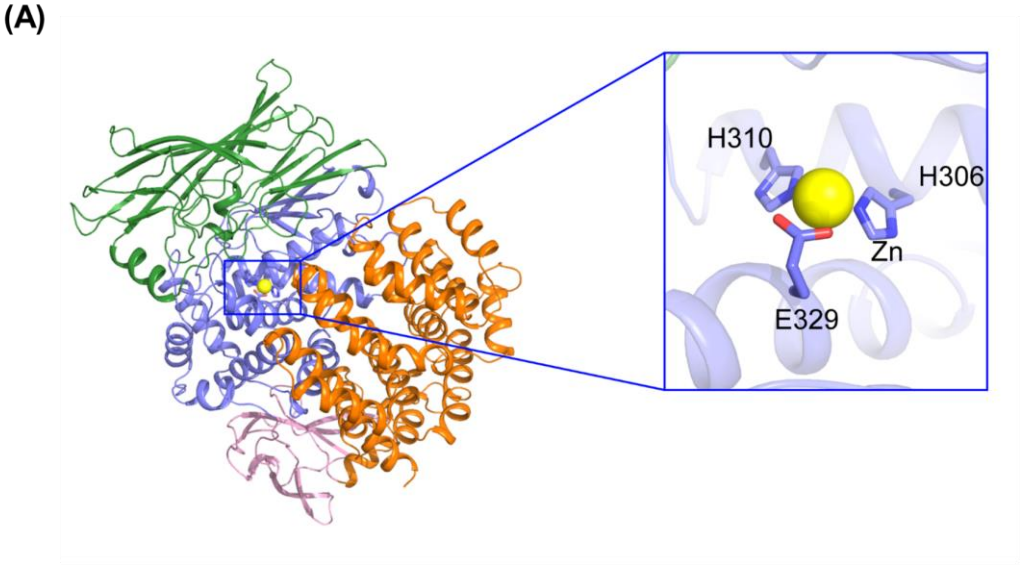


**Supplementary Figure 6.** EryP contains a zinc binding motif that is highly conserved in M1 Zn-dependent metallopeptidases. (A) The overall crystal structure of EryP and the close-up view of the Zn binding residues. (B) Sequence alignment of EryP with M1 Zn-dependent metallopeptidases. Catalytic residues are labeled with stars and the conserved HEXXH$(X)_{18}$E is highlighted. Accession numbers of related proteins: EryP(WP_009950696.1), AplP(AHB63590.1), ePepN(AAA24317.1), ERAP1(NP_001185470.1).

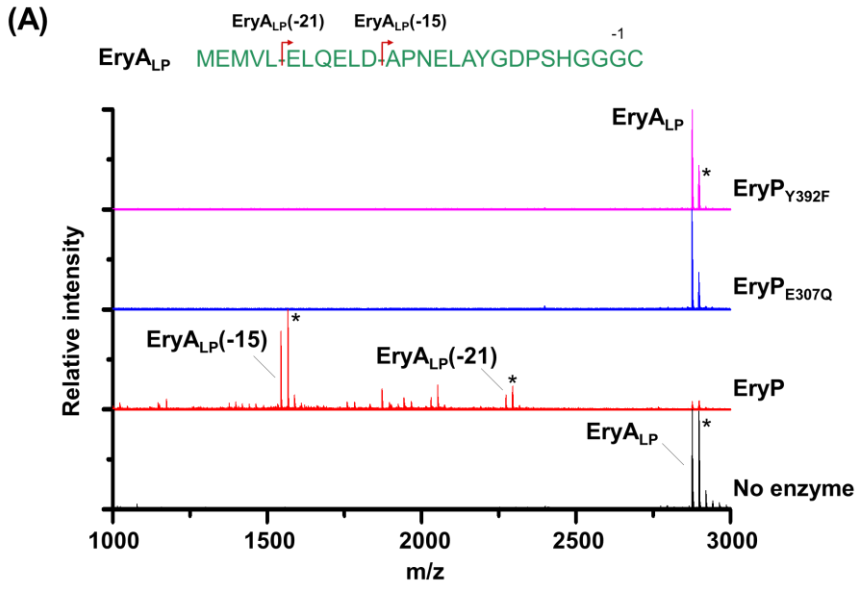


| Species | Sequence | Predicted Mass/Da | Observed Mass/Da |
|---|---|---|---|
| EryA$_{LP}$(-15) | APNELAYGDPSHGGGC | 1544.62 | 1544.76 |
| EryA$_{LP}$(-21) | ELQELDAPNELAYGDPSHGGGC | 2271.98 | 2272.17 |
| EryA$_{LP}$ | MEMVLELQELDAPNELAYGDPSHGGGC | 2876.18 | 2876.33 |

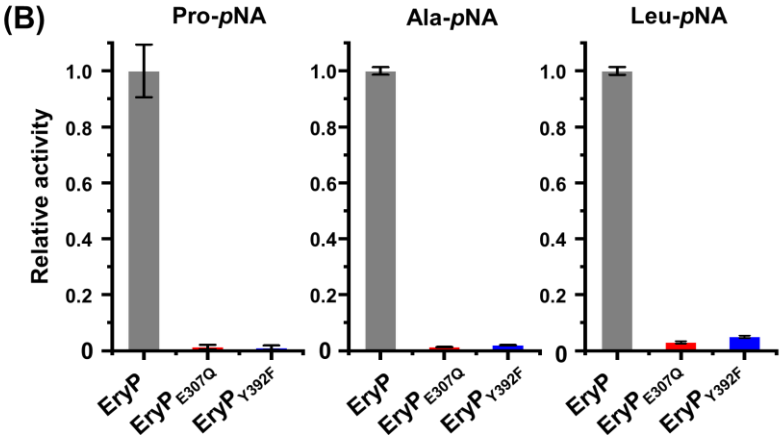


**Supplementary Figure 7.** Both endopeptidase and aminopeptidase activities of EryP$_{E307Q}$ and EryP$_{Y392F}$ were abolished. (A) EryP$_{E307Q}$ and EryP$_{Y392F}$ were inactive toward EryA$_{LP}$ peptide. Assay conditions: 100 μM EryA$_{LP}$ peptide and 1.0 μM EryP were incubated in 20 mM Tris buffer, *p*H 8.0, at 37 °C for 24 h. (B) The aminopeptidase activity of EryP$_{E307Q}$ and EryP$_{Y392F}$ toward amino acid *p*NA derivatives were almost abolished compared with EryP. * represents the sodium adducts of peptides in MS. Error bars indicate standard deviation of three independent replicates.

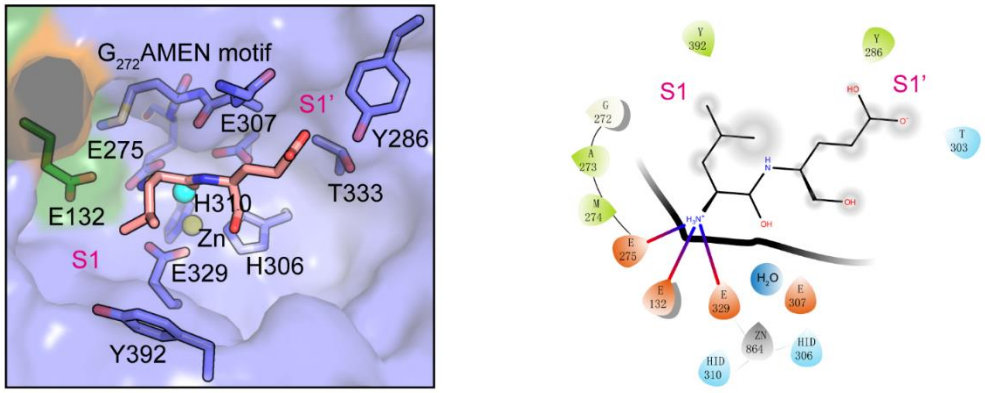


**Supplementary Figure 8.** The docking model of a dipeptide Leu-Glu into the active site of EryP in the *closed* state. Following the convention for naming peptidase sites, the site responsible for accommodating the peptide side chain N-terminal to the cleavage site is named **S1**, and the subsequent position are named **S1′**.

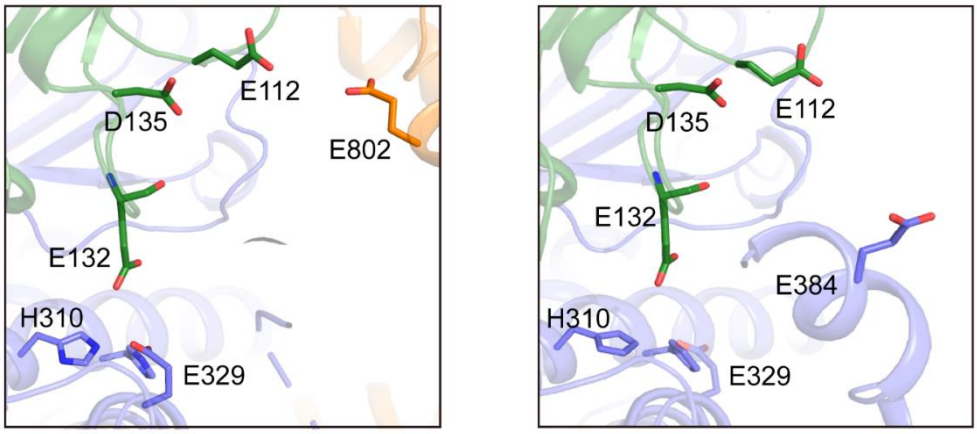


**Supplementary Figure 9.** The Ca binding residues in the *intermediate* and *open* states of EryP.

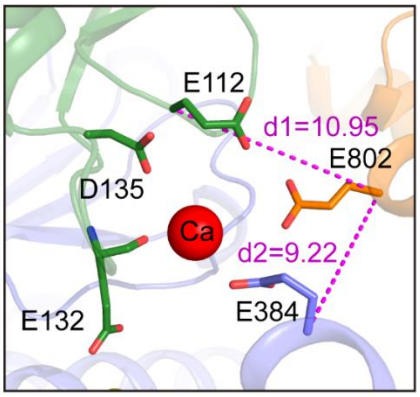


**Supplementary Figure 10.** Dimensional descriptors were selected to describe the motion of domain-IV relative to domain-I and II: **d1** is the distance between the CA atoms of E802 and E112, and **d2** is the distance between the CA atoms of E802 and E384. In the *closed* state of EryP, **d1** = 10.95 Å and **d2** = 9.22 Å.

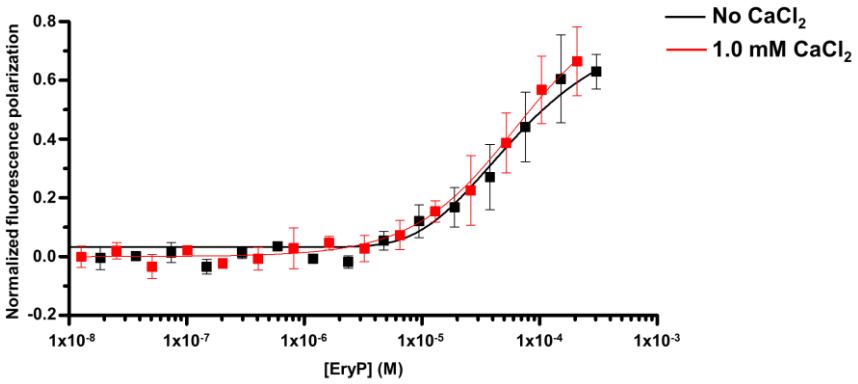


**Supplementary Figure 11.** The binding affinity of EryP with $EryA_{LP}$ was not altered by the addition of 1.0 mM $CaCl_2$. $K_D$ values for EryP-$EryA_{LP}$ binding are 52.9±11.5 μM (no $CaCl_2$) and 59.8±7.9 μM (1.0 mM $CaCl_2$). Error bars indicate standard deviation of three independent replicates.

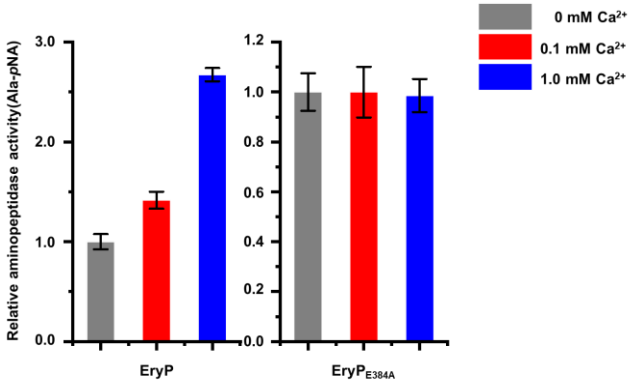


| | Velocity (μM·min$^{-1}$) | |
|---|---|---|
| [$CaCl_2$] | EryP | $EryP_{E384A}$ |
| none | 0.55 ± 0.04 | 1.0 ± 0.1 |
| 0.1 mM | 0.78 ± 0.05 | 1.0 ± 0.1 |
| 1.0 mM | 1.5 ± 0.1 | 0.99 ± 0.07 |

**Supplementary Figure 12.** The aminopeptidase activity of $EryP_{E384A}$ toward Ala-*p*NA was not responsive to the change of $Ca^{2+}$ concentration. Assay conditions: EryP or $EryP_{E384A}$ (1.0 μM) was incubated with Ala-*p*NA (0.10 mM) in 20 mM Tris buffer, *p*H 8.0, at 37 °C. Error bars indicate standard deviation of three independent replicates.

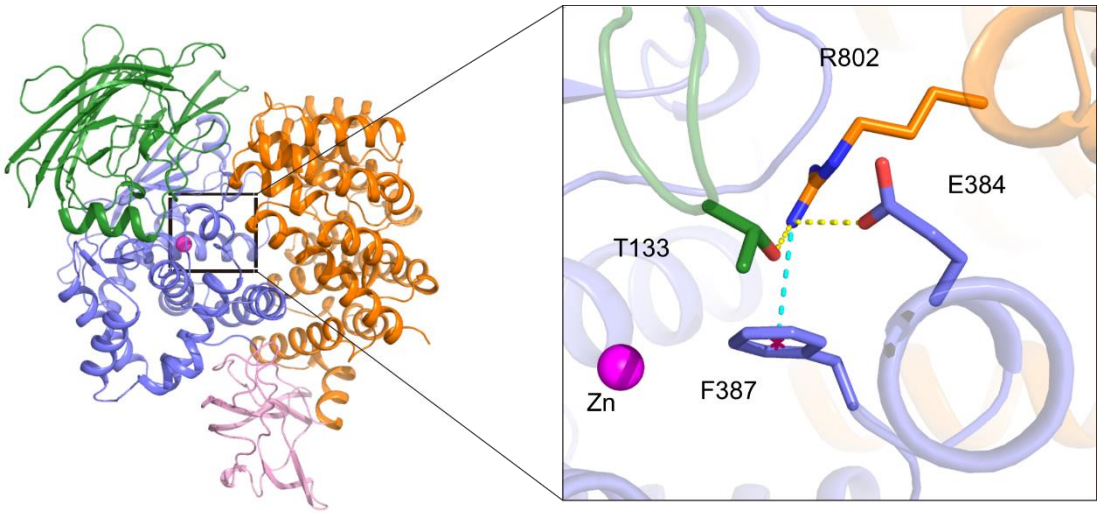


**Supplementary Figure 13.** The overall crystal structure of $EryP_{E802R}$ and the close-up view of the inter-domain interactions between residues T133, E384, F387 and R802.

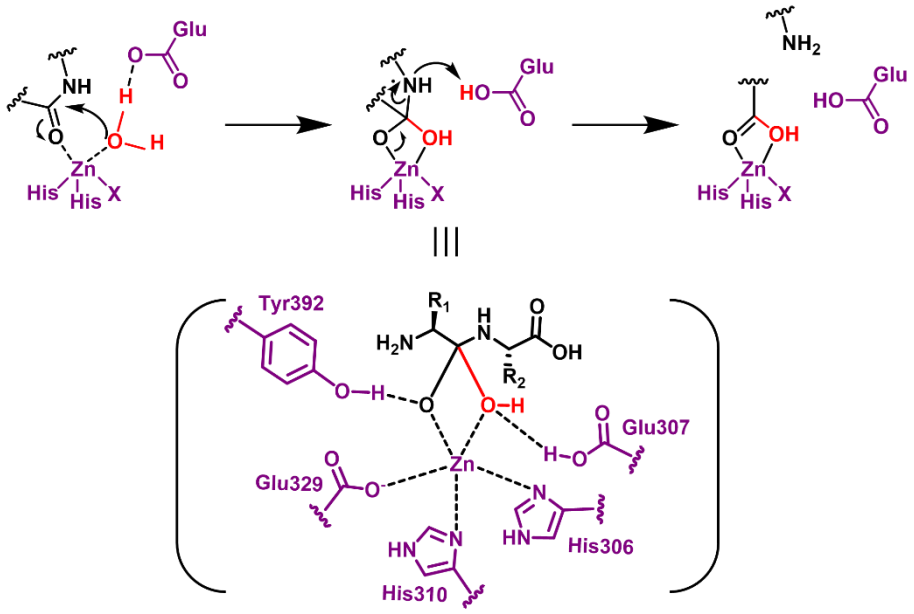


**Supplementary Figure 14.** Y392 stabilizes the tetrahedral intermediate during enzymatic amide hydrolysis.

| Substrate | Enzyme | [$CaCl_2$] | $K_m$(mM) | $V_{max}$(μM·$min^{-1}$) | $k_{cat}$($min^{-1}$) | $k_{cat}/K_m$ ($min^{-1}$·$mM^{-1}$) | Relative |
|---|---|---|---|---|---|---|---|
| **Ala-*p*NA** | EryP | none | 36 ± 5 | 81 ± 9 | 81 | 2.2 | 1.0 |
| | $EryP_{E802R}$ | none | 0.57 ± 0.05 | 22 ± 1 | 1075 | 1876 | 837 |
| | | 1.0 mM | 0.27 ± 0.01 | 12 ± 1 | 575 | 2148 | 954 |
| **Leu-*p*NA** | EryP | none | 1.6 ± 0.1 | 18 ± 1 | 18 | 11 | 1.0 |
| | $EryP_{E802R}$ | none | 0.23 ± 0.02 | 38 ± 1 | 1890 | 8169 | 748 |
| | | 1.0 mM | 0.22 ± 0.01 | 32 ± 1 | 1599 | 7129 | 653 |

**Supplementary Figure 15.** $EryP_{E802R}$ displays significantly improved aminopeptidase activity and is not responsive to the presence of Ca ions. Kinetic parameters are acquired from Michaelis-Menten analysis of EryP and $EryP_{E802R.}$ Assay conditions: 20 mM Tris buffer, *p*H 8.0, 1.0 μM EryP or 0.02 μM $EryP_{E802R}$. The concentration of amino acid-*p*NA derivatives ranges from 10 μM to 10 mM. Error values indicate standard deviation of three independent replicates.

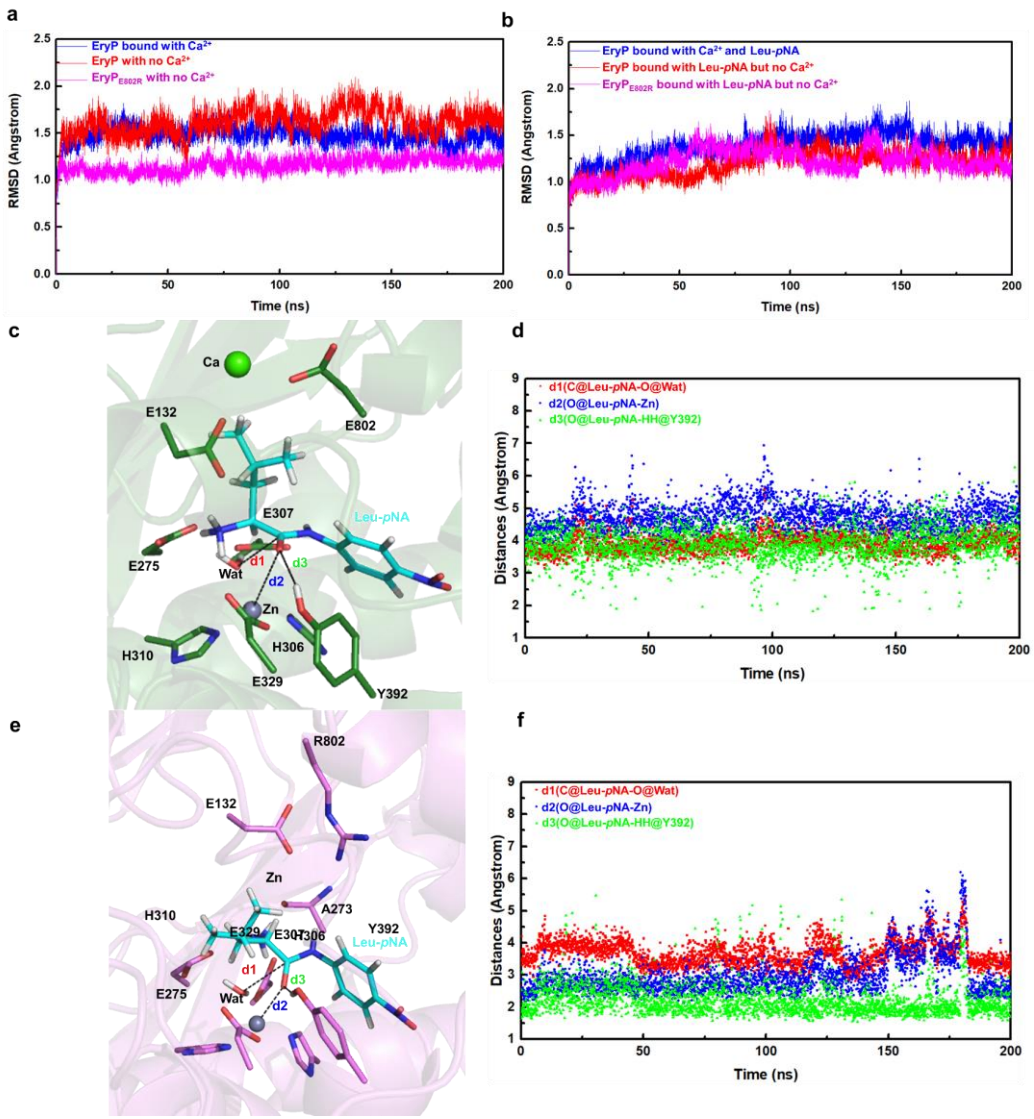


**Supplementary Figure 16.** RMSD of backbone heavy atoms relative to the first snapshot during 200 ns classical MD simulation on (**a**) EryP and $EryP_{E802R}$ with or without Ca ions and (**b**) EryP-(Leu-*p*NA) and $EryP_{E802R}$-(Leu-*p*NA) complexes with or without Ca ions. According to the RMSDs, all MD trajectories reaches equilibrium and the protein structures are dynamically stable. Representative MD snapshot and key distances of (**c**-**d**) EryP-(Leu-*p*NA) in complex with $Ca^{2+}$ and (**e**-**f**) $EryP_{E802R}$-(Leu-*p*NA) in complex without $Ca^{2+}$ during 200 ns MD simulations.

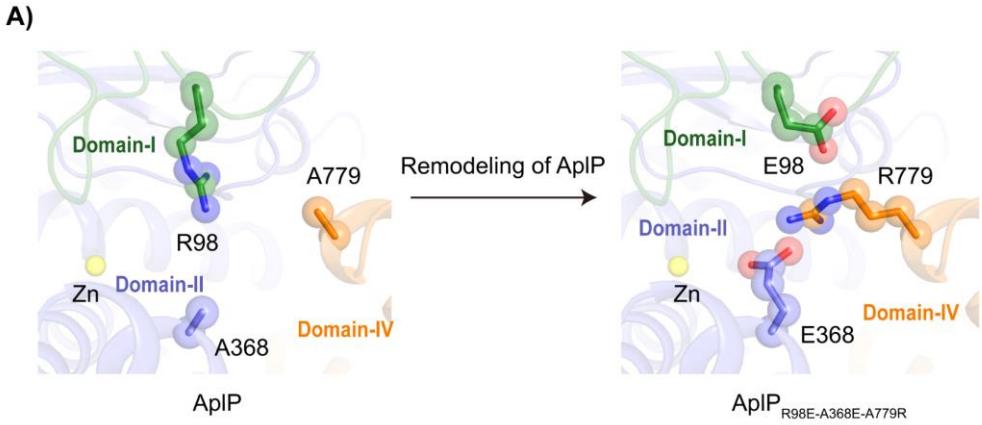


**Supplementary Figure 17.** Residues R98, A368 and A779 in the modeled AplP structure, and the designed inter-domain charge-charge interaction in $AplP_{R98E\text{-}A368E\text{-}A779R}$.

| | **Velocity（μM·min$^{-1}$）** |
|---|---|
| **AplP** | 0.65 ± 0.03 |
| **$AplP_{R98E\text{-}A368E\text{-}A779R}$** | 1.7 ± 0.1 |
| **Relative** | 2.6 |

**Supplementary Figure 18.** The aminopeptidase activity of $AplP_{R98E\text{-}A368E\text{-}A779R}$ was enhanced by 2.6-fold compared with AplP toward Ala-*p*NA. Assay conditions: 1.0 μM AplP or $AplP_{R98E\text{-}A368E\text{-}A779R}$ was incubated with 100 μM Ala-*p*NA in 20 mM Tris buffer, *p*H 8.0, at 37 °C. Error values indicate standard deviation of three independent replicates.

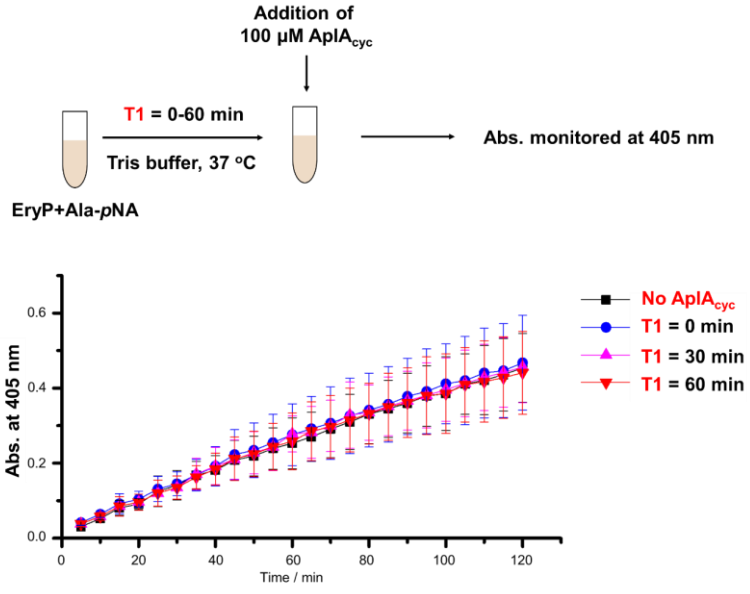


**Supplementary Figure 19.** The hydrolysis of Ala-*p*NA by EryP was not accelerated by the addition of peptide substrate $AplA_{cyc}$. Assay conditions: 10 μM EryP was incubated with 1.0 mM Ala-*p*NA in 20 mM Tris buffer, *p*H 8.0, at 37 °C for **T1** min before 100 μM $AplA_{cyc}$ peptide was

added in the reaction mixture. The absorbance at 405 nm was monitored after the addition of $AplA_{cyc}$. Error bars indicate standard deviation of three independent replicates.

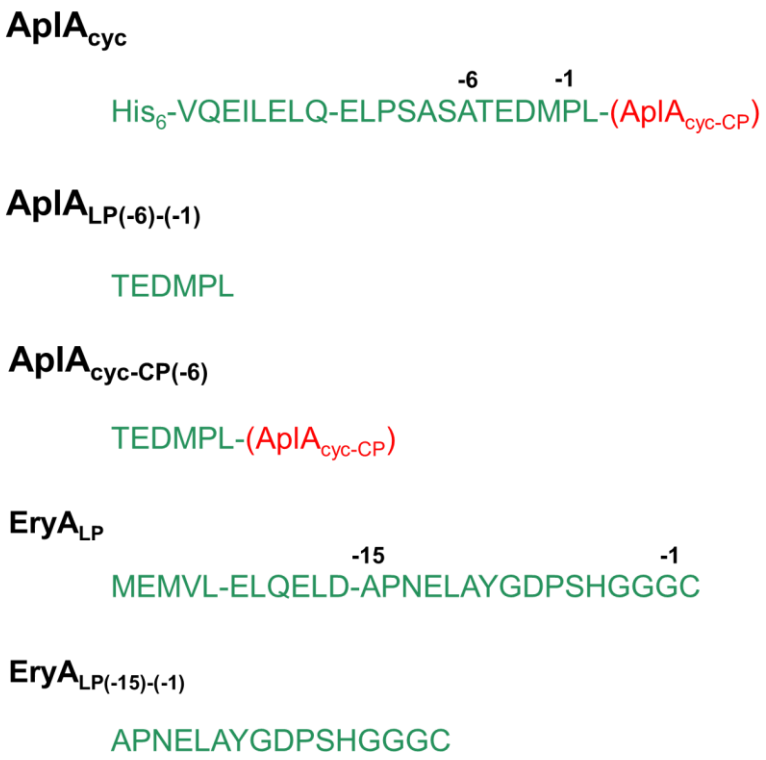


**Supplementary Figure 20.** Sequences of peptide substrates.